Proceedings of the National Seminar & Exhibition
on Non-Destructive Evaluation
NDE 2011, December 8-10, 2011

AN EMAT-BASED SHEAR HORIZONTAL (SH) WAVE TECHNIQUE FOR ADHESIVE BOND INSPECTION

K. Arun[a], R. Dhayalan[a], Krishnan Balasubramaniam[a], Bruce Maxfield[a], Patrick Peres[b] and David Barnoncel[b]
[a]Centre for Nondestructive Evaluation, Indian Institute of Technology Madras, Chennai INDIA
[b]Astrium Space Transportation, EADS, Av du Général Niox – BP 20011, FRANCE.

ABSTRACT

The evaluation of adhesively bonded structures has been a challenge over the several decades that these structures have been used. Applications within the aerospace industry often call for particularly high performance adhesive bonds. Several techniques have been proposed for the detection of disbonds and cohesive weakness but a reliable NDE method for detecting interfacial weakness (also sometimes called a kissing bond) has been elusive. In particular, ultrasonic methods, including those based upon shear and guided waves, have been explored for the assessment of interfacial bond quality. Since some of the 3-D guided shear horizontal (SH) wave modes in plates have predominantly shear displacement at the plate surfaces, we conjectured that SH guided waves should be influenced by interfacial conditions when they propagate between adhesively bonded plates of comparable thickness. This paper describes further developments of a new technique based on SH guided waves that propagate within, are reflected from and which propagate through a lap joint. Through mechanisms we are beginning to understand, the propagation of an SH wave through a lap joint gives rise to a reverberation signal that is due to one or more reflections of an SH guided wave mode within that lap joint. Based upon a combination of numerical simulations and measurements, this method shows promise for detecting and classifying interfacial bonds. It is also apparent from our measurements that some of the SH wave modes can discriminate between adhesive and cohesive bond weakness in both Aluminum-Epoxy-Aluminum and Composite-Epoxy-Composite lap joints. All measurements reported here used periodic permanent magnet (PPM) Electro-Magnetic Acoustic Transducers (EMATs) to generate either or both of the two lowest order SH modes in the plates that comprise the lap joint. This exact configuration has been simulated using finite element (FE) models to describe the SH mode generation, propagation and reception. Of particular interest is that one SH guided wave mode (probably SH0) reverberates within the lap joint. Moreover, in both simulations and measurements, features of this so-called reverberation signal appear to be related to interfacial weakness between the plate (substrate) and the epoxy bond. The results of a hybrid numerical (FE) approach based on using COMSOL to calculate the EMAT driving forces within an elastic solid and ABAQUS to propagate the resulting elastic disturbances (waves) within the plates and lap joint are compared with measurements of SH wave generation and reception in lap joint specimens having different interfacial and cohesive bonding conditions.

Keywords **:** EMAT, Adhesive bond inspection, metals, composites, Finite Element Model, Shear Horizontal, Ultrasonic Wave.
PACS: 62.20.De, 81.05.Ni, 87.57.Nf **PACS:** 62.20.De, 81.05.Ni, 87.57.Nf

INTRODUCTION

Adhesive bonds are used extensively in the manufacture of structures. They are particularly common throughout the aerospace industry. The strength and performance of these bonds, often in the form of lap joints, is frequently critical to the performance of structures that incorporate them. In particular, lap joints in aerospace structures must be designed to withstand high loads. Hence, one key role of NDE in these structures is to classify defects within these bonds. Defects of interest include disbonds, weak interfacial bonding between the adhesive and one surface of the lap joint (sometimes referred to as a kissing bond), cohesive weakness within the bond itself and defects such as foreign material within the adhesive or on one of the surfaces.

Shear horizontal (SH) wave guided modes in 3-D structures have predominantly shear displacements. Because of this, SH plate modes are expected to be sensitive to the coupling between two plates when each plate can support the particular SH mode. For the case of a lap joint between two essentially identical plates, it was postulated that SH wave energy propagating from one plate into the other would be influenced by the properties of the adhesive bonding layer joining the

two plates. As described in more detail below and as generally expected, elastic energy in the SH0 mode flows from one plate into the other (from plate 1 into plate 2 in Figure 1). When the lap joint bond is "good," there is very efficient coupling of elastic energy through the joint; this feature is evident in both simulations and measurements. Also expected is a reflection from the end of plate 1 back toward the SH wave source; this is also present in the simulations and measurements. An unexpected result, present in both simulations and measurements, is the appearance of what we refer to as a reverberation signal. Based upon following the signal evolution in the simulations, this signal appears to be due to a reflection from the right end of plate 1 that is subsequently reflected from the left end of plate 2.

All measurements were made with the T and R EMATs at equivalent positions on each of the four 3 mm thick specimens, as shown in Fig. 1. The T and R EMATs were positioned directly facing each other. Identical EMATs were used for both T and R functions. Although good signal-to-noise ratios have not yet been achieved with a small "line" receiver EMAT, it is clear that discrimination of the reverberation signal is enhanced with these receivers (a line receiver is one that responds to surface shear displacements over a portion of the SH beam width but only for a small fraction of a wavelength in the direction of beam propagation). For measurements reported here, the T and R EMATs were positioned as shown. A-scans were recorded for a few T EMAT locations. The left (plate 1) and right (plate 2) plates were each 250 mm long with a 50 mm wide overlap region (darkened region in the Figure 1).

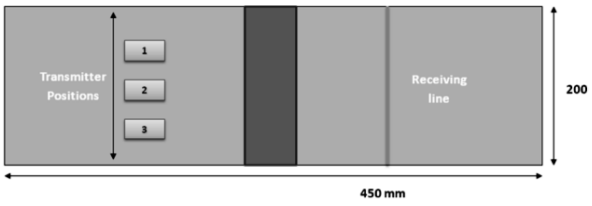

Fig. 1 : Geometry of the specimens reported here with the position of the Transmitters (T) and Receivers (R) as shown. Plate 1 is on the left.

The remainder of this paper describes the essential features of our measurements and simulations as well as some conclusions that appear reasonable based upon both measurement and simulation.

PPM SH EMATS

PPM SH EMATs based upon previous designs were used for all measurements reported here [1 to 8]. The T EMAT was positioned to generate an SH wave propagating generally parallel to the long direction of the plate (see Figure 1). A reasonable compromise between time/spatial resolution and sensitivity required that the T EMAT be only 2 or 3 wavelengths long and about the same width. This configuration has the disadvantage of rather large beam spread (consequently, SH modes will not be incident normally over the entire right end of plate 1). As discussed later, this can influence mode conversion when an SH mode is reflected from a plate end.

PPM SH EMATs were used to generate the SH0 mode in plate 1 and to detect what was predominantly the SH0 mode that was coupled into plate 2. To date, two sets of cases have been evaluated. The first was a set of measurements and corresponding simulations of aluminum-epoxy-aluminum lap joints as shown in Figure 1. Preliminary measurements have also been made on lap joints in epoxy-bonded carbon fiber composite plates. In this case, SH waves were generated using adhesive-backed Al tape bonded to the composite surface. These lap joints present a different and more complex set of conditions for both measurements and simulations. A complete presentation of these results will be the subject of another paper.

Identical T and R EMATs, each 2.5 wavelengths long, were constructed and placed on lap joint specimens as indicated in Fig. 2. All measurements reported here were made in the through-transmission geometry. Measurements were made on four, 3 mm thick lap joint specimens (measurements were also made on lap joints fabricated from 8 mm thick Al; the points we wish to emphasize here are most clear for the thinner metallic specimens). Simulations were done for conditions identical to the measurement configuration. The R EMAT signal is proportional to the SH displacement profile integrated over the R EMAT reception area (this has been demonstrated in many different measurement geometries [2, 3, 5, 7]. The measurement geometry was identical for the four cases. The difference in bonding was represented in the numerical calculations by using different elastic properties for the adhesive for part or all of the lap joint region. Damping in the

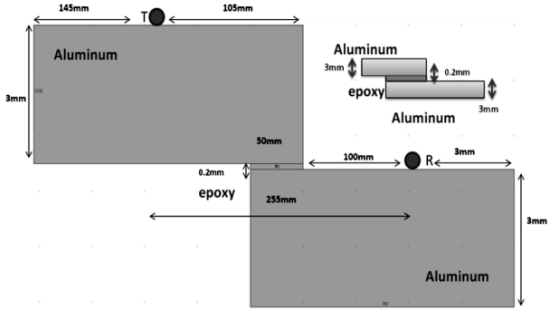

Fig. 2 : The detailed measurement configuration for the Al specimens. Identical positions and plate dimensions were used for all measurements and for calculating the simulated A-scans. The T and R EMATs were of identical construction. The composite plates were of similar construction.

adhesive is not considered in this work but is elsewhere. Calculation details are also given elsewhere. Actual frequencies used for the measurements reported here range from 140 kHz to 300 kHz. The excitation pulse is shaped by a Hanning window

SIMULATION OF SH WAVE MODES

A two-step procedure was chosen for doing these simulations because it contains most of the physics of the problem while lending considerable simplicity to the numerical work.

Although some measurement features are not contained in this approach, the fact that most detailed features of the EMAT signals appeared in the simulations gives us confidence that this procedure is a very good approximation to understanding the origin of features in the measured EMAT signals.

This two-step procedure first used a COMSOL FEMLAB formulation of the 2-D approximation of the surface current generated by the EMAT coil and the PPM magnet configuration to calculate the electromagnetic force on and within the metal surface (the force distribution within the first few skin depths in the aluminum). This results in being able to assign an excitation force to each of the mesh nodes in the subsequent elasto-dynamic calculation. These are the driving forces for elastic wave excitation in the plate. The 3-D finite element elasto-dynamic model ABAQUS was used to calculate the elastic disturbance resulting from the applied electro-dynamic forces. It should be noted that ABAQUS calculates the 3 orthogonal displacements that result from the exciting force distribution. The exciting force generated by the 3-D EMAT coil is taken as the set of 2-D electro-dynamic forces calculated in the surface region immediately beneath the EMAT coil and magnets and zero elsewhere (more details related to these calculations have been presented elsewhere [9]). In this manner, it is possible to obtain a surface shear displacement as a function of time at any point, along any line or over any area on the material surface. This displacement (averaged over the R EMAT coil active area) generates the amplitude-time or A-scan signal received by the R EMAT.

COMPARISON OF SIMULATIONS WITH MEASUREMENTS FOR AL LAP JOINTS

Numerical and experimental studies were done for the following four aluminum specimens; all were 3 mm thick plates with a 50 mm overlap darkened bonded region in Fig. 1. In the description below, the following designations are used; (i) specimen 8129: fabricated to have a known good bond, (ii) specimen 8182: made with epoxy that was contaminated with silicon, (iii) specimen 8181: made with a soft adhesive and (iv) specimen 8183: the only specimen that was made without abrasively polishing (sanding) both surfaces in contact with the adhesive. The composite lap joint specimen was the same thickness, of identical geometry and had a "good" bond.

An illustrative snapshot of an SH wave simulation is given below in Fig. 3 for specimen 8183. The lack of sanded surfaces was accounted for in the simulation by using a weaker interfacial force between the epoxy and the (assumed oxidized) Al surface. The first (direct through-transmission) signal received by the R EMAT propagates in plate 1 through the lap

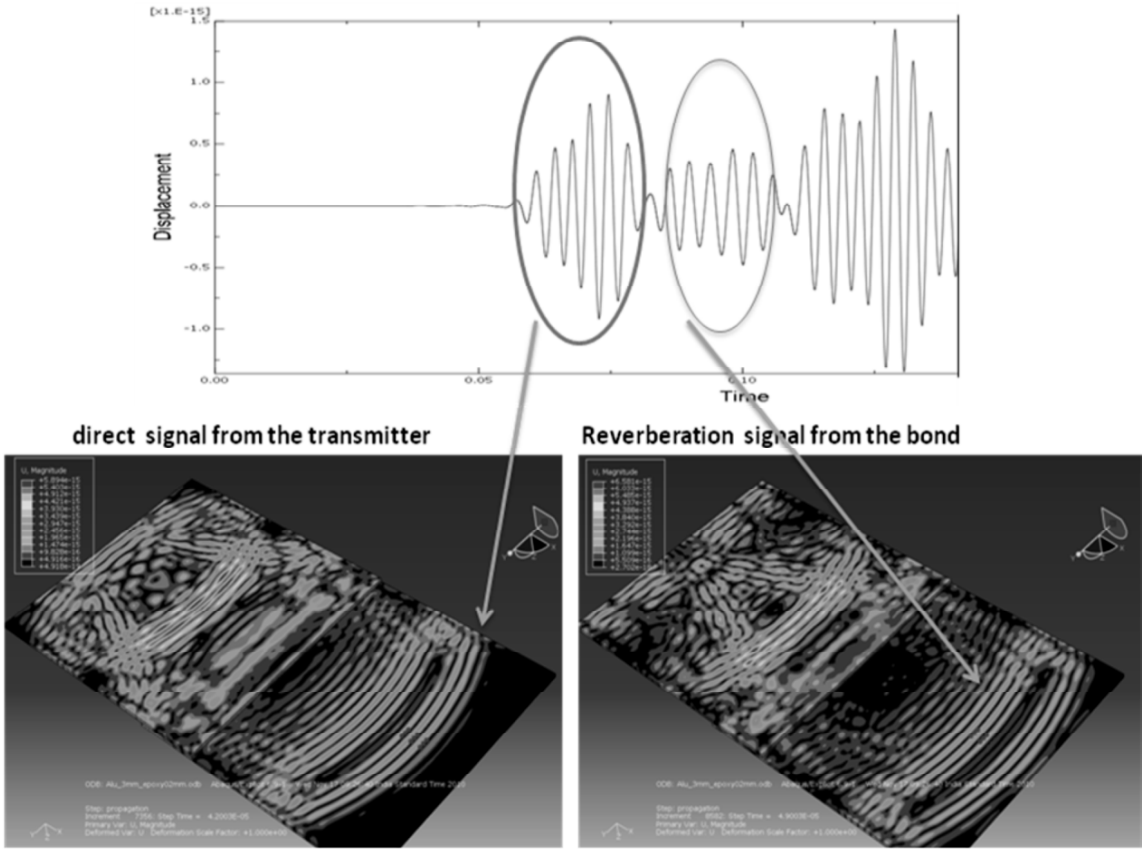

Fig. 3 : The direct and reverberated SH0 signals obtained using the ABAQUS FEM model showing (a) the A-scan at a specific point (red region on plate 2), and (b) surface displacement map obtained using ABAQUS.

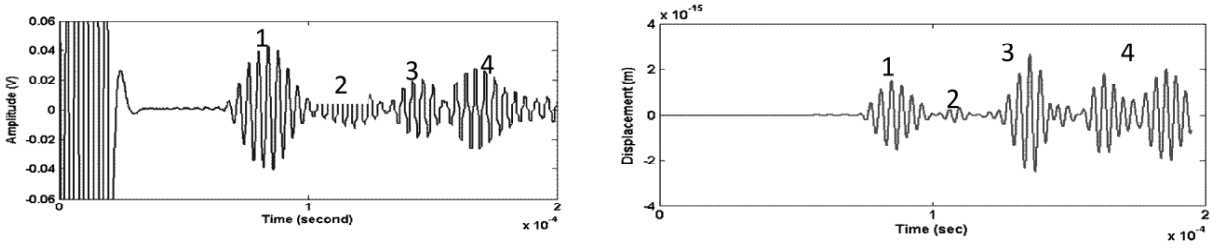

Fig. 4 : Comparison between experimentally obtained signals from the lap joint sample 8129 (good bonded sample) with the simulated signal obtained using the ABAQUS FEM model showing the (1) Direct SH0 Signal, (2) Reverberated SH0 signal, (3 and 4) reflections from the ends.

joint and is received in plate 2 (see Fig. 2). The second signal is interpreted as resulting first from a reflection off the right end of plate 1 and then the left end of plate 2 where it is reflected toward and received by the R EMAT. The time between the first two signals corresponds to an SH0 mode being reflected from plate 1 and then plate 2 to the receiver. The last set of signals in Fig. 3 is a combination of reflections from the left end of plate 1 and the right end of plate 2 reaching the receiver in the same time range.

Fig. 4 compares measurement and simulation for the well-bonded specimen, 8129. Probably because the assumed bonding conditions for the simulations did not represent the actual bond, the measured amplitude ratio for the direct-to-reverberation signal is larger in the simulation. Of particular note is that both the direct and reverberation signals are very distinct. Not shown here are the results for an epoxy bond polluted by a silicone adhesive; here, both the direct and reverberation signals are much lower in magnitude, presumably because of attenuation within the lap joint. While the time of arrival of the different modes compare well, the amplitudes do not. The direct-to-reverberation signal ratio is larger for both measurement and simulation than in the well-bonded case.

EFFECT OF BOND QUALITY ON THE REVERBERATED SH0 SIGNAL

The Fig. 5 shows the amplitude of the SH0 reverberated signal amplitude at 5 different positions (distance from one of the sides across the 200 mm wide sample) showing that the reverberated SH0 signal for the weak interface samples (8181 and 8183) is lower when compared to the good interface conditions as in the samples 8129 and 8182. It was also determined that the weak adhesive sample 8182 showed a significanly lower direct signal when compared to the other samples.

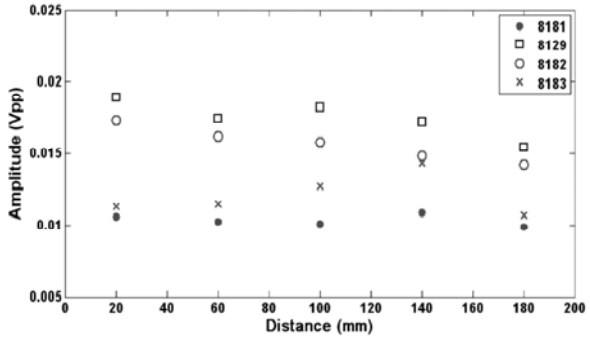

Fig. 5 : Comparison of experimentally obtained reverberated signal amplitudes for the lap joint sequence measured at different T-R positions across the lap joint.

CONCLUSIONS

In this work, the EMAT based SH0 guided wave generation and transmission across a lap joint made of Al-Epoxy-Al was studied using both Finite Element Models and experimental studies. The generation of a direct and a reverberated signal from within the lap joint was observed and confirmed using FEM animations. These two signals were found to be sensitive to both the cohesive and adhesive propoerties of the adhesive bond. The direct signal was found to be useful in identifying the cohesively weak bonds while the reverberated signal was found to be more sensitive to the interfacial weakness conditions. The reverberated SH0 signal may provide a new technique for the detection of weak adhesion during manufature and in-service inspection of adhesively bonded structures.

REFERENCES

1. B.W. Maxfield, Kuramoto A, Hulbert JK, *Evaluating EMAT designs for selected applications.* Mater. Eval., 1987; 45(10):1166–83.
2. R.B. Thompson, *Physical principles of measurements with EMAT transducers*, In: Thurston RN, Pierce AD, editors. Physical acoustics, 19. San Diego: Academic Press; 1990.
3. B. W. Maxfield and C. M. Fortunko, *The design and use of electromagnetic acoustic wave transducers (EMATs)*, Mater. Evul., vol.41, pp. 1399-1408, NOV. 1983.
4. G. A. Alers and L. R. Bums, *EMAT designs for special applications*, Mater. Evul., vol. 45, pp. 1184-1189, Oct. 1987.
5. R. Ludwig, Z. You, R. Palanisamy, *Numerical simulation of an electromagnetic acoustic transducer–receiver system for NDT applications*, IEEE Trans. Magnet. 29 (1993) 2081–2089.

6. R. J. Shapoorabadi, A. N. Sinclair, and A. Konrad, *Finite element determination of the absolute magnitude of an ultrasonic pulse produced by an EMAT*, in 2000 IEEE Int. Ultrasonics Symp., Puerto Rico, October 2000.
7. X. Jian, S. Dixon, S.R. Edwards, *Optimal ultrasonic wave generation of EMAT for NDE,* Non-Destruct. Eval. (2005) 42–62.
8. M. Hirao and H. Ogi, *EMATs for Science and Industry-Noncontacting Ultrasonic measurements,* Kluwer Academic Publishers, 2003.
9. R. Dhayalan, K. Balasubramaniam, *A hybrid finite element model for simulation of Electro-magnetic Acoustic transducer (EMAT) based plate waves*, NDT&E International, 43 (2010) 519-526.
10. T.J. Moran and R.M. Panos, *Electromagnetic generation of electronically steered ultrasonic bulk waves*, J. Appl. Phys, Vol.47, No.5, May 1976.
11. R. Ludwig and X.-W. Dai, *Numerical simulation of electromagnetic acoustic transducer in the time domain,* J. Appl. Phys, vol. 69, pp. 89-98, 1991.
12. B. Dutton, S. Boonsang, R.J. Dewhurst, *A new magnetic configuration for a small in-plane electromagnetic acoustic transducer applied to laser-ultrasound measurements: Modeling and validation*, Sensors and Actuators A 125 (2006) 249–259.
13. R. Ludwig, *Theoretical basis for a unified conservation law description of the electromagnetic acoustic transduction process,* IEEE Trans. Ultason., Ferroelec. Freq. Contr., vol. 39, pp. 476-480, July 1992.
14. R. J. Shapoorabadia and A. Konradb, *The governing electrodynamic equations of electromagnetic acoustic transducers,* Journal of Applied Physics 97, 10E102 (2005).
15. R. J. Shapoorabadia, A. Konradb and A. N. Sinclair, *Improved Finite Element Method for EMAT Analysis,* IEEE Trans. Magnet. Vol. 37, No. 4, July 2001.
16. J.K. Hu, Q.L. Zhang and D.A. Hutchins, *Directional characteristics of electromagnetic acoustic transducers,* Ultrasonics, Vol No.26, January 1988.
17. W. J. Pardee and R. B. Thompson, *Half-Space Radiation by EMATs,* Journal of Nondestructive Evaluation, Vol 1, No. 3, 1980.
18. S. Soua, A. Raude, and T-H. Gan, *Guided Wave in Engineering Structures Using Non-Contact Electromagnetic Acoustic Transducers – A Numerical Approach for the Technique Optimisation*, Excerpt from the Proceedings of the COMSOL Conference 2009, Milan.